Environmental Science & Technology

pubs.acs.org/est

Article

# Prioritizing the Best Potential Regions for Brine Concentration Systems in the USA Using GIS and Multicriteria Decision Analysis

Rodrigo A. Caceres Gonzalez and Marta C. Hatzell*

Cite This: https://doi.org/10.1021/acs.est.2c05462

Read Online

ACCESS | Metrics & More | Article Recommendations | Supporting Information

**ABSTRACT:** We propose a methodology for identifying and prioritizing the best potential locations for brine concentration facilities in the contiguous United States. The methodology uses a geographic information system and multicriteria decision analysis (GIS-MCDA) to prioritize the potential locations for brine concentration facilities based on thermodynamic, economic, environmental, and social criteria. By integrating geospatial data with a computational simulation of a real brine concentration system, an objective weighting method identifies the weights for 13 subcriteria associated with the main criteria. When considering multiple dimensions for decision making, brine concentration facilities centered in Florida were consistently selected as the best location, due to the high second-law efficiency, low transportation cost, and high capacity for supplying municipal water needs to nearby populations. For inland locations, Southeast Texas outperforms all other locations for thermodynamic, economic, and environmental priority cases. A sensitivity analysis evaluates the consistency of the results as the priority of a main criterion varies relative to other decision-making criteria. Focusing on a single subcriterion misleads decision making when identifying the best location for brine concentration systems, identifying the importance of the multicriteria methodology.

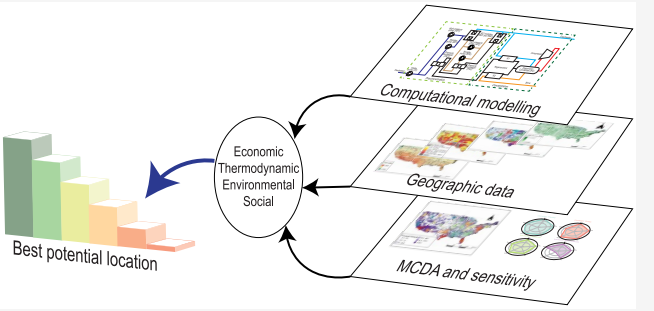


**KEYWORDS:** *GIS, MCDA, desalination, MLD, brine concentration, computational modeling, Shannon entropy*



## INTRODUCTION

Water scarcity today affects approximately 40% of the world's population[1] and may double by 2050.[2] Industrial-scale desalination is rapidly growing as the most reliable strategy to produce clean water from unconventional water sources to augment global water supplies. As of 2022, there are ∼13600 desalination plants online, presumed online, and under construction worldwide. These plants have a total capacity of 100 million cubic meters of freshwater per day. By 2030, it is anticipated that this will increase to 122 million cubic meters of freshwater per day (from current planned and awarded plants). This equates to a growth in the desalination industry by 22% over the next eight years.[3] The majority (91%) of these plants treat seawater and brackish water and operate with an average recovery ratio of 42%.[3,4] Thus, for every cubic meter of freshwater produced, the desalination industry rejects 1.38 $m^3$ of a higher-concentration brine. Only 1% of the current desalination plants treat brine or concentrated seawater, and thus most is rejected as waste.[3] As this new industry grows, emphasis on sustainable decision making is critical to prevent additional impacts to the environment.[5]

Commercial brine management strategies are limited to sewer discharge, surface water discharge, deep-well injection, and evaporation ponds.[6] In a rare case, brine is reused for irrigation. Rejecting waste brine to local water reservoirs without proper management can impact local ecosystems, which is a strong motivator for developing technologies and facilities which can treat this waste rather than dispose waste.[7] However, beyond waste production, the disposal of conveyed water away from a desalination site is energy intensive and counterproductive. Thus, state of the art brine management strategies do not mitigate risks and result in a significant loss of valuable water.[6]

Minimal liquid discharge (MLD) and zero liquid discharge (ZLD) desalination plants are emerging as the ideal approach to both minimize brine rejection and disposal and maximize water recovery.[8−10] MLD desalination systems achieve a recovery ratio of up to ∼95% depending on feed salinity. With this operation for every cubic meter of water produced, only 0.05 $m^3$ of water is wasted. Furthermore, ZLD desalination plants achieve a recovery ratio of ∼99%, resulting in no wasted water. The output waste for MLD is a low-volume salt-saturated brine and for ZLD is a solid salt. A

**Special Issue:** Data Science for Advancing Environmental Science, Engineering, and Technology

**Received:** July 29, 2022
**Revised:** November 21, 2022
**Accepted:** November 22, 2022

traditional ZLD system combines a preconcentrator system (e.g., typically reverse osmosis) with a thermal-based system as a brine concentrator. The most common and mature brine concentrator method is mechanical vapor compression (MVC).[8,11] A crystallizer or evaporation pond can further separate the water from the concentrated brine. Most MLD/ZLD investigations focus on the development of new technologies such as forward osmosis, or solvent extraction, and new evaporative methods using renewable energies as the energy driver.[12−18] There is also an interest in the improvement of existing membrane-based technologies.[19−21] However, these methods are not in a commercial state. Regarding commercial and available technologies, success is evaluated traditionally through optimization of a single criterion (e.g., energy and/or cost). However, the practical feasibility of MLD/ZLD systems at a large scale will also depend on social and geographic criteria, which are often neglected.[1,4,22−27] Thus, a thorough evaluation of the feasibility of MLD and ZLD facilities requires analyses that can evaluate the performance, cost, and environmental constraints simultaneously. Multicriteria decision analysis (MCDA), which has gained interest as a multidisciplinary decision-making tool for sustainable systems, allows one to take into consideration several criteria at the same time to generate the best decisions and solutions.[28] In desalination, MCDA allows for identifying the potential best technology for specific locations based on environmental, technical, and economic criteria.[29,30] When it is integrated with geospatial data, MCDA allows for identifying the potential and suitability of a determined location or regions for implementing a desalination system.[22,31−35]

Here, we propose a multicriteria decision analysis which combines a computational thermodynamic model with a geographic information system to identify the potential and prioritize regions for brine concentration facilities operating under minimum liquid discharge (MLD plants). Identification of the best potential geographic location is based on thermodynamic, economic, environmental and social criteria (Figure 1). The establishment of brine concentration facilities and networks throughout the contiguous United States ultimately will aid in minimizing waste and maximizing water production from industrial desalination processes.

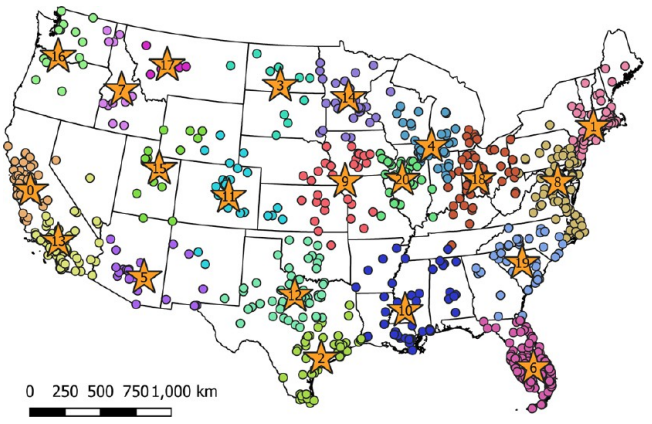


**Figure 1.** Centroid for treating brine rejected by desalination plants as identified by the K-means algorithm. Dots represent the location of a desalination plant, and the color represents the assigned cluster.

## METHODOLOGY

**Computational Model of Brine Concentration System.** The brine concentration system evaluated for this investigation hybridizes the most mature technologies available for achieving minimum liquid discharge (Figure 2). The exhaust of the hybrid system produces a saturated brine (260 g/kg) and can achieve a recovery ratio up to 96%: i.e, it is a MLD system.[8,36] Hybridization increases the total recovery ratio, allowing for the production of high-concentration brine and minimal or zero liquid discharge. Hybridization reduces the total specific energy consumption in comparison to the nonhybrid counterpart. This is accomplished through combining the most efficient technologies for a specific feed salinity in series.[37]

In the preconcentration stage, the effluent brine from the closest desalination plants mixes and becomes the feedwater entering the intake pump. In the first pressure exchanger (PX1), 60% of the feedwater flows, exchanging pressure with the residual brine from the second pressure exchanger (PX2), and then flows through the booster pump (BP1) for mixing with the remaining 40% of the feedwater from a high-pressure pump (HP1) before entering the first RO module (RM1). In the second pressure exchanger (PX2), 60% of the brine from the first RO module flows, exchanging pressure with the residual brine from the second RO module, and then flows through the booster pump (BP2) for mixing with the remaining 40% of brine from the second high-pressure pump (HP2) before entering the second RO module (RM2). In every RO module, the flow is divided equally to flow into several units composed of 43 pressure vessels with 7 membrane elements each. The brine from the second RO module is transported into both pressure exchangers as a high-pressure fluid and into the regenerators (R1 and R2) as a low-temperature fluid. The number of RO units inside the RO modules depends on the amount of feed treated. Each unit treats 2000 $m^3$/h. In the concentration step of the evaluated system, the brine enters the evaporator, where vapor from the compressor transfers heat to drive the evaporation process. The condensed vapor mixes with the permeate from the RO modules to provide freshwater to nearby locations. A saturated brine (260 g/kg of concentration) leaves the evaporator/condenser as the effluent brine of this system. A crystallizer or evaporation pond can further treat this concentrated brine (Figure S4).

The thermodynamic model is evaluated in an engineering equation solver (EES),[38] which evaluates energy, mass, and concentration balances across each component and system. The primary outputs from the thermodynamic model are LCOW, specific energy consumption (SEC), specific entropy generation, total freshwater−water produced, total brine rejected, recovery ratio, specific area used for the evaporator in the MVC subsystem, and system second-law efficiency.[39−45] Brine thermophysical properties, assumed to be an aqueous sodium chloride solution, are estimated from published data sets and developed correlations.[46−50] The governing equations of the computational model and validation are available in the Supporting Information.

*System Metrics.* The 13 metrics/subcriteria estimated by the computational model and geographic data are the second-law efficiency ($\eta_{II}$), recovery ratio (RR), specific energy consumption (SEC), specific entropy generation ($s_{gen}$), levelized cost of water (LCOW), transportation cost of intake


https://doi.org/10.1021/acs.est.2c05462
Environ. Sci. Technol. XXXX, XXX, XXX−XXX

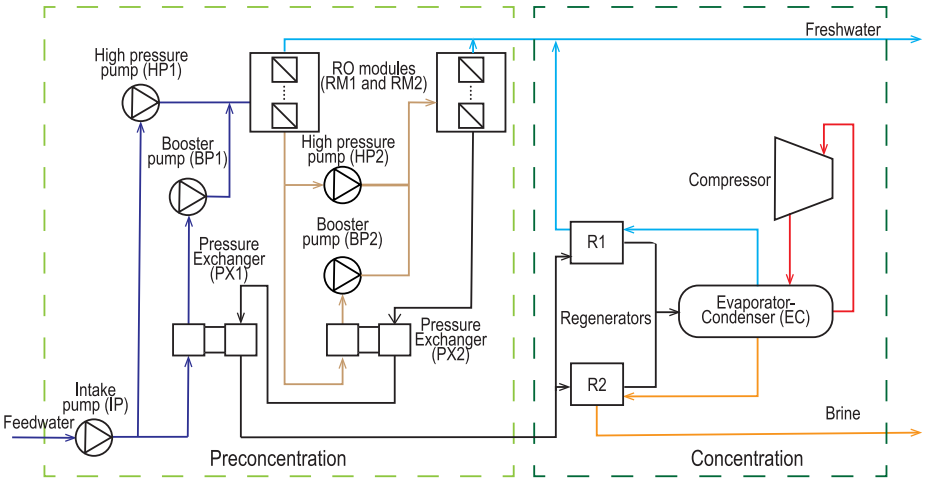


**Figure 2.** Diagram for the integrated two-stage RO (light green dased box) and single-effect MVC (dark green dased box) subsystems working as a brine concentrator. The incoming water (feedwater) is preconcentrated in the RO system to be further concentrated until saturation (260000 PPM) in the MVC system. The total freshwater−water produced is the combination of the product streams of every subsystem (light blue line). On average, the concentration of the freshwater produced by the system, according to the computational model, is 0.57 g/kg.

and supply ($\text{Trnsprt}_{\text{intake}}$ and $\text{Trnsprt}_{\text{supply}}$), $CO_2$ emissions ($CO_2$) associated with the operation of the plant, specific area of the MVC evaporator/condenser (SA), percentage of water supplied to nearby major cities ($\%_{\text{supply}}$), annual average global horizontal irradiation (GHI), water stress, and land cost (land). GHI, water stress, and land are obtained directly from raster data and do not require further calculations.

Second-law efficiency relates the minimal possible energy consumption with the actual consumption as[36,43]

$$\eta_{\text{II}} = \frac{\text{SEC}_{\text{min}}}{\text{SEC}_{\text{system}}} \tag{1}$$

where $\text{SEC}_{\text{min}}$ is the thermodynamic minimum energy of separation as a function of concentration and recovery ratio[43]

$$\text{SEC}_{\text{min}} = 2 \cdot R \cdot T_{\text{f}} \cdot \left[ \frac{C_{\text{f}}}{M_{\text{NaCl}} \cdot \text{RR}} \cdot \ln\left(\frac{C_{\text{b}}}{C_{\text{f}}}\right) - \frac{C_{\text{d}}}{M_{\text{NaCl}}} \cdot \ln\left(\frac{C_{\text{b}}}{C_{d}}\right) \right] \tag{2}$$

where $R$ is the universal gas constant, $T_{\text{f}}$ is the feed temperature, $M_{\text{NaCl}}$ is the molar mass of sodium chloride (58.44 g/mol), and $C_{\text{f}}$, $C_{\text{b}}$, and $C_{\text{d}}$ are the concentrations of the feed, brine and product, respectively. RR is the recovery ratio defined as the ratio between the produced water ($m_{\text{d}}$) and the feed ($m_{\text{f}}$):

$$\text{RR} = \frac{m_{\text{d}}}{m_{\text{f}}} \tag{3}$$

The specific energy consumption of the system ($\text{SEC}_{\text{system}}$) considers the total amount of freshwater produced ($m_{\text{fresh,system}}$) and the total electrical energy consumption

$$\text{SEC}_{\text{system}} = \frac{\dot{W}_{\text{RO}} + \dot{W}_{\text{C}}}{m_{\text{fresh,system}}} \tag{4}$$

where $\dot{W}_{\text{RO}}$ is the total energy consumption of the RO subsystem operating as preconcentrator, equal to the summation of the high-pressure and booster pumps ($\dot{W}_{\text{HP},pump,1}$, $\dot{W}_{\text{booster,pump,1}}$, $\dot{W}_{\text{HP,pump,2}}$, and $\dot{W}_{\text{booster,pump,2}}$) in the RO subsystem (Figure 2), and $\dot{W}_{\text{C}}$ is the total energy consumption of the compressor in the mechanical vapor compression subsystem operating as a brine concentrator:

$$\dot{W}_{\text{RO}} = \dot{W}_{\text{raw,pump,1}} + \dot{W}_{\text{HP,pump,1}} + \dot{W}_{\text{booster,pump,1}} + \dot{W}_{\text{HP,pump,2}} + \dot{W}_{\text{booster,pump,2}} \tag{5}$$

The energy consumption of the compressor is a function of the pressure change in the device and the suction temperature as[40]

$$\dot{W}_{\text{C}} = \frac{m_{\text{v}} \cdot c_{\text{p,v}} \cdot T_{\text{C,in}}}{\eta_{c}} \cdot (\text{PR}^{\gamma_{\text{v}}-1/\gamma_{\text{v}}} - 1) \tag{6}$$

where $m_{\text{v}}$ and $c_{\text{p,v}}$ are the flow and specific heat of the vapor in the compressor at the suction temperature $T_{\text{C,in}}$, respectively. PR is the pressure ratio in the compressor and $\eta_{\text{c}}$ the compressor efficiency, assumed to be 0.7.[40]

The specific entropy generation ($s_{\text{gen}}$) considers the total entropy generation of the brine concentration system and the total freshwater production ($m_{\text{fresh,system}}$)

$$s_{\text{gen}} = \frac{\dot{S}_{\text{gen,RO}} + \dot{S}_{\text{gen,MVC}}}{m_{\text{fresh,system}}} \tag{7}$$

where $\dot{S}_{\text{gen}}$ represents the total entropy generation and the subscripts RO and MVC indicate the subsystem.

The levelized cost of water of the system considers the total annualized cost of the RO and MVC subsystem and the annual production of the plant

$$\text{LCOW} = \frac{\text{TAC}_{\text{RO}} \cdot 1.03 + \text{TAC}_{\text{MVC}}}{m_{\text{fresh,system}} \cdot \text{hours} \cdot 365 \cdot f_{\text{c}}} \tag{8}$$

where $\text{TAC}_{\text{RO}}$ and $\text{TAC}_{\text{MVC}}$ are the total annualized costs of the RO and MVC subsytems, respectively. The 1.03 factor represents a conservative difference between a traditional RO system and one working as high pressure-reverse osmosis (HPRO), where the top pressure increases up to 120 bar.[51] The total annualized cost is the summation of the annual operational cost and the annualized capital cost (ACC) as follows:


https://doi.org/10.1021/acs.est.2c05462
Environ. Sci. Technol. XXXX, XXX, XXX−XXX

$$TAC = ACC + \sum OC \tag{9}$$

$$ACC = CC \cdot \frac{CEPCI_{2021}}{CEPCI_{2000}} \cdot CRF \tag{10}$$

The annualized cost is corrected to year 2021 with the CEPCI correction factor using as a reference the year 2000.[52−54] The CEPCI values for 2000 and 2021 are 394.1 and 750, respectively. CRF is the capital recovery factor used for annualizing the capital costs of the subsystem

$$CRF = \frac{i \cdot (1 + i)^{LF}}{(1 + i)^{LF} - 1} \tag{11}$$

where $i$ is the interest rate, assumed to be 0.05, and LF the lifetime of the plant, assumed to be 20 years.[44]

The transportation cost considers the cost of the pumping energy required to transport the water to the potential site of the brine concentration plant and to the nearby cities[55]

$$\dot{W}_{p,trnsprt} = \frac{Pump_{HP} \cdot 0.7457}{\eta_{p,t} \cdot \eta_m} \tag{12}$$

where $\eta_{p,t}$ and $\eta_m$ are the pump and motor efficiencies, respectively, assumed to be 0.9 and 0.95. The pump horsepower ($Pump_{HP}$) depends on the elevation and friction head as

$$Pump_{HP} = \frac{Flow_{rate} \cdot (Friction_{head} + Elevation_{head})}{3956} \tag{13}$$

where the friction head is function of the distance and flow properties, while the elevation head is obtained through geographical data[56]

$$Friction_{head} = \frac{Moody_{FF} \cdot d \cdot Velocity^2}{2 \cdot diameter \cdot g} \tag{14}$$

where $Moody_{FF}$ is the Moody friction factor, $d$ the Euclidean distance, and $g$ the gravity constant. The transportation cost refers to the cost of pumping the water to its destiny

$$Trnsprt_{intake} = \frac{\dot{W}_{p,trnsprt,intake} \cdot 8760 \cdot energy_{cost,c}}{m_{feed,system}} \tag{15}$$

$$Trnsprt_{supply} = \frac{\dot{W}_{p,trnsprt,supply} \cdot 8760 \cdot energy_{cost,c}}{m_{fresh,system}} \tag{16}$$

where the subscript "intake" represents the process of pumping the brine from nearby desalination plants to the brine concentration plant and the subscript "supply" represents the process of pumping the produced water into nearby cities. $energy_{cost,c}$ represents the average energy grid cost in the state where the centroid c is located.

$CO_2$ emissions depend on the carbon intensity of the location selected and the specific energy consumption:

$$CO_2 = Carbon_{intensity} \cdot SEC_{system} \tag{17}$$

Carbon intensity depends on the state of analysis (Table S16). The national average value in 2018 was 0.18 kg/kWh with values ranging from 0.12 to 0.27 kg/kWh[57]

The specific area of the MVC evaporator/condenser depends on the heat transfer area and the total produced water

$$SA = \frac{A_{PH} + A_{EC}}{m_{fresh,system}} \tag{18}$$

where $A_{PH}$ is the heat transfer area of the regenerators (R1 and R2) operating as preheaters and $A_{EC}$ the heat transfer area of the evaporator/condenser in the MVC subsystem operating as brine concentrator.

The percentage of water supplied to nearby major cities is a function of the produced freshwater per system, the total population density assigned to every centroid, and the total water consumed for indoor home use

$$Supply_{\%} = \frac{m_{fresh,system}}{0.0142 \cdot Population_{total,c}} \tag{19}$$

where 0.0142 ($m^3/h$) is the average water consumption per person for indoor home use[58] and $Population_{total,c}$ is the summation of the population of every major city assigned to the plant located in the centroid c.

**GIS Analysis.** A geographic information system (GIS) analysis uses quantitative spatial data regarding the location of current desalination plants in the contiguous USA (Figure S2). The application of a distance based K-means clustering algorithm agglomerates the current desalination plants in the contiguous US into potential regions where the brine concentration system is evaluated.[59] The mean coordinate of every cluster (the centroid point) represents the location for the brine concentration plant for further analysis. These plants receive the total brine rejected from the nearest desalination plants belonging to the same cluster (Figure 1). A mass and concentration balance estimate the feed flow ($m^3/h$) and concentration of the saline effluent from nearby desalination plants (equations are available in the Supporting Information). The brine concentration system provides freshwater to nearby major cities and produces a saturated brine ready for crystallizing.

The geospatial data considered in the GIS approach consist of the daily average global horizontal irradiance (GHI), water stress level, land cost, terrain elevation, electricity prices, carbon intensity, and location and population of the nearby major cities.[56,57,60−64] The lack of complete geographical data for Alaska and Hawaii (Elevation, GHI, water stress level, and land cost), restrict this study to only the contiguous USA.

**Multicriteria Decision Analysis.** The 4 main criteria determined from the model are thermodynamic, economic, environmental, and social. Within the 4 main criteria, we further define 13 subcriteria. Each subcriterion influences the prioritization of the locations for installing a brine concentration plant. The thermodynamic subcriteria include the second-law efficiency ($\eta_{II}$), plant recovery ratio (RR), specific energy consumption (SEC) in $kWh/m^3$, and specific entropy generation ($s_{gen}$) in $kW/(K\ m^3/d)$.

The economic subcriteria include the levelized cost of water (LCOW) in $\$/m^3$, land cost (Land) in log($/ha), the cost of transporting the brine for the desalination plants into the centroid ($Trsp_{intks}$), and the transport cost for distributing the produced freshwater to the nearby major cities ($Trsp_{supp}$) both in $\$/m^3$. Transportation costs are relevant if the total distance exceeds 250 miles. In this case, the energy intensity can surpass the total energy requirements for freshwater production in a RO system.[55] Thus, placement of a brine concentrating system must be within 250 miles to ensure that the transportation


https://doi.org/10.1021/acs.est.2c05462
Environ. Sci. Technol. XXXX, XXX, XXX−XXX

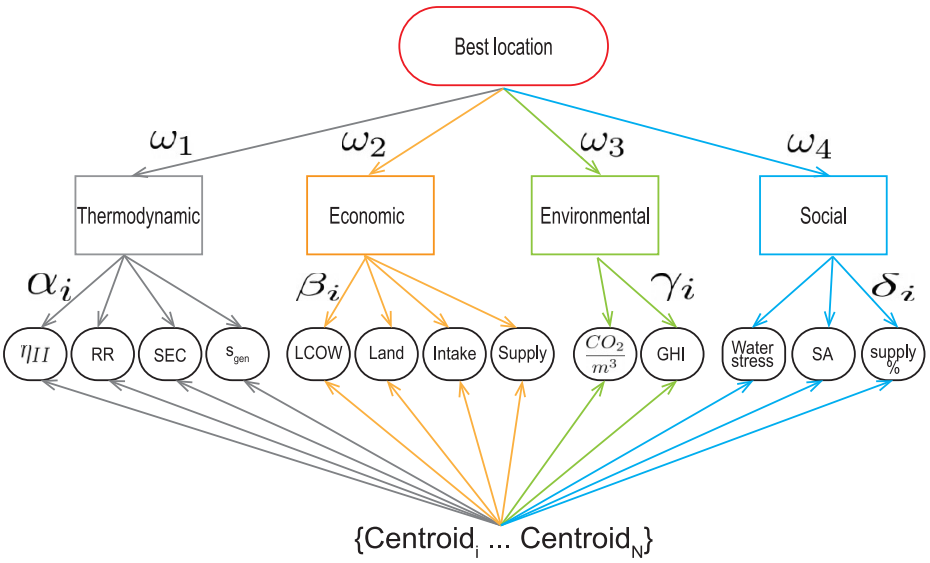


**Figure 3.** Multicriteria decision analysis layer of decision to identify the centroid representing the best location. There are 4 main criteria, thermodynamic (gray arrows), economic (orange arrows), environmental (green arrows), and social (light blue arrows) aspects, subdivided into 13 subcriteria.

energy does not exceed the specific energy consumption for treatment.

The environmental subcriteria include the $CO_2$ emissions of the plant in kg $CO_2/(m^3\ d)$ and the GHI of the location in $kW/(m^2\ d)$. The social subcriteria include water stress levels, specific area of the MVC subsystem (SA) in $m^2/m^3$, and the percentage of freshwater demand that the brine concentration plant can supply to the nearby cities ($Supply_{\%}$). The heat transfer area of the MVC subsystem is more relevant when it is compared with the RO module plant area. This is due the fact that, to produce 1 kg of freshwater, the entropy generation of the evaporator/condenser in the MVC system is about 5 times higher than the entropy generation in the RO module.[39,41] The heat transfer area of the evaporation is directly dependent on the amount of freshwater produced; a large heat transfer area allows for producing more water but increases the entropy generation.[39] On the other hand, RO module entropy generation is a direct function of the pressure drop through the membrane and the change in concentration during permeation.[39] A larger operational pressure requires less pressure vessels in the RO module, decreasing the area and size.[65] The GIS analysis assigns the closest cities to a centroid based on the nearest distance.

A multicriteria decision analysis (MCDA) using the technique for order of preferences by similarity to ideal solution (TOPSIS) method ranks every centroid location based on the 4 main criteria and 13 subcriteria (Figure 3). The TOPSIS method is an accepted method for sustainable decision making, based on multiple criteria and objectives.[66,67] This method identifies, based on Euclidean distance, the closest alternative to the best positive solution while being far from the negative solution.[68] The simplicity of this method allows TOPSIS to be used to evaluate multidisciplinary problems and systems (e.g., desalination).[30,32,69,70] The TOPSIS method considers the following steps (detailed equations are provided in the Supporting Information):

1. construction of decision matrix with alternatives represented by the potential locations, criteria, and subcriteria
2. normalization of decision matrix
3. multiplication of normalized decision matrix by the weights of the criteria and subcriteria
4. determination of positive and negative ideal solutions
5. estimation of distance of each alternative from positive and negative ideal solutions
6. Estimation of closeness coefficient per alternative. Closeness coefficient indicates the relative closeness to the positive ideal solution and distance to the negative ideal solution.
7. Rank of alternatives based on closeness coefficient

A crucial requirement in the TOPSIS method is the weight assignation for every criterion ($\omega_1$–$\omega_4$) and subcriterion ($\alpha_i$, $\beta_i$, $\gamma_i$, and $\delta_i$) composing every layer of decision (Figure 3). The multiplication of the local weight of every subcriterion by its main criterion weight provides the global weight of every subcriterion. The global weights of the subcriteria are multiplied by the normalized decision matrix in the TOPSIS method.

Five cases represents possible priority distributions for the main criteria weights values ($\omega_j$). The equal priority case (Eq) assigns the same weight to every main criterion ($\omega_1 = \omega_2 = \omega_3 = \omega_4 = 0.25$), indicating than none of the main criteria have a preference among the others. The thermodynamic priority case (Th) assigns a weight of 0.5 to the thermodynamic criterion ($\omega_1 = 0.5$) and distributes equally the remaining 0.5 into the other three criteria ($\omega_2 = \omega_3 = \omega_4 = \frac{0.5}{3}$). The economic priority case (Ec) assigns a weight of 0.5 to the economic criterion ($\omega_2 = 0.5$) and distributes equally the remaining 0.5 into the other three criteria (($\omega_1 = \omega_3 = \omega_4 = \frac{0.5}{3}$). The environmental priority case (Env) assigns a weight of 0.5 to the environmental criterion ($\omega_3 = 0.5$) and distributes equally the remaining 0.5 into the other three criteria ($\omega_1 = \omega_2 = \omega_4 = \frac{0.5}{3}$). The social priority case (Soc) assigns a weight of 0.5 to the social criterion ($\omega_4 = 0.5$) and distributes equally the remaining 0.5 into the other three criteria ($\omega_1 = \omega_2 = \omega_3 = \frac{0.5}{3}$). The priority cases aims to evaluate


https://doi.org/10.1021/acs.est.2c05462
Environ. Sci. Technol. XXXX, XXX, XXX−XXX

the influence of assigning a high important to one specific criterion based on potential preferences of decision makers.

The Shannon entropy weighting method provides the weights for every subcriterion ($\alpha_i$, $\beta_i$, $\gamma_i$, and $\delta_i$).[71] This method is based on the information theory and indicates that the entropy of a data set can provide information about the quality and quantity of data needed for reliable decision making. The entropy method is a data-based weighting method suitable for avoiding the judgment or subjectivity of decision makers when undesired or available.[35] The lower the entropy of a subcriterion, the higher its diversity/discriminability ($1 - E_j$).[72] A subcriterion with low entropy or large diversity provides more useful information (reduced uncertainty) and, therefore, has a higher weight.[68,73−76] A detailed estimation of the entropy index is available in the Supporting Information.

This GIS-MCDA weighted by the Shannon entropy weighting method allows for an objective prioritization of the potential locations for the brine concentration plants, combining geospatial data and computational modeling results.

## RESULTS AND DISCUSSION

The clustering process groups all reported desalination plants within the contiguous USA into 21 clusters (Figure 1). The desalination plants within each cluster operate with different desalination technologies and feedwater quality (Figure S2). The majority of the desalination plants in the United States operate with reverse osmosis (RO) systems (subfigure at the bottom in Figure S2) and treat brackish water (subfigure at the top in Figure S2). Only nine desalination plants treat brine as the main feedwater source. The majority of the brine treatment sites operate with a thermal-based desalination system (e.g., multieffect distillation (MED), multistage flash distillation (MSF), or mechanical vapor compression (MVC)).

The total brine produced at each desalination plant within a cluster serves as the inlet feedstream to the brine concentration plant, which is located in the centroid. Every cluster has a unique number and code (see Table S6). The average distance between a desalination plant and the centroid where the brine concentration plant would be located is 169 km. The maximum distance is 539 km with a third quartile value Q3 of 218 km. This ensures that the transport distance from desalination plants to the brine concentration plant is below 250 miles (~400 km). This condition is held for ~75% of the cases. As mentioned in Methodology, 250 miles is a critical threshold for the conveyance of water. When a conveyance distance exceeds 250 miles, the energy consumption during transport exceeds the energy required to produce water.[55] For every brine concentration plant, the computational thermodynamic model and the geographic data available calculate 13 subcriteria (Table S7) related to thermodynamic, economic, environmental, and social criteria. Twenty-one is the best selected number of clusters provided by the analysis using the elbow method. The addition of more clusters did not improve the performance of the clustering algorithm, as the mean distance from every point to its cluster (represented as the sum of squared errors) with 22 clusters is not significant different from that with 21 clusters (Figure S6). The 21 value is not located directly in the elbow, but there is a negligible change in the sum of squared errors of the clustering algorithm after this number. Increasing the number of clusters may also produce the selection of isolated clusters (i.e. clusters composed by only one desalination plant). This is due the limitations of the K-means algorithm employed in this work, where the agglomeration criterion only considers the location of every desalination plant.

**Subcriterion Performance for Brine Concentration Plants.** For the thermodynamic criterion (Table S8), the second-law efficiency ranges from 8% to 19% with an average efficiency of 13%. This second-law efficiency is similar to those of conventional thermal concentrator systems and a single-stage standalone MVC.[77,78] In desalination, the second-law efficiency provides a measure of how optimally the system separates the salt from the water, in comparison with an thermodynamically ideal system. Specifically, the second-law efficiency compares the minimal energy required for separation (estimated through the Gibbs energy difference) with the actual exergy input of the system. The use of exergy allows for a fair comparison for all the energy inputs of a system. This is imperative when comparing different locations for a brine concentration system.

The SEC ranges from 11 to 13.5 kWh/m$^3$. As expected, this SEC is higher than that of conventional seawater membrane-based desalination systems (e.g., seawater RO) but is lower than that of seawater thermal-based desalination systems (MED or MSF). State of the art brine concentrator system total equivalent energy consumption ranges from from 10 to 35 kWh/m$^3$.[79] The RO-MVC studied system average SEC is 50% lower than the energy consumption of a standalone MVC concentrating the same amount and quality of brine.

For the economic criterion (Table S9), the LCOW ranges from 0.9 to 2 with an average of 1.5 \$/m$^3$. The LCOW is higher than conventional brine disposal methods such as surface water and sewer discharge (0.4−0.8 \$/m$^3$) but is comparable with those of deep-well injection (2−2.8 \$/m$^3$), irrigation and land application (1.2−1.6\$/m$^3$), and reported thermal brine concentrators or salt separators (Figure S3).[6,77] The average LCOW is also lower than that of standalone seawater thermal desalination systems, and the minimum value is comparable with that of a standalone seawater RO.[80] The minimal LCOW attained is in the range proposed by the USA government for nonconventional water sources, indicating that brine concentration facilities may be able to reach pipe parity.[81] Transportation cost, either intake from nearby desalination plants or supply to nearby population, has an average value of below 0.1 \$/m$^3$. The maximum transportation costs of the intake and supply are equal to 34% and 37% of the LCOW, respectively. Therefore, locations selected as centroids by the GIS analysis are viable, since the transportation cost and energy demand are not higher than the water production cost and energy demand.

For the environmental criterion (Table S10), $CO_2$ emission ranges from 1.6 to 3.1 kg $CO_2$/(m$^3$ d) with an average of 2.3. This range is lower than the estimated emissions for the current desalination industry (25 kg $CO_2$/m$^3$).[37,82] The brine concentration system uses electricity for most operations (e.g. pumps in the RO subsystem and a compressor in the MVC subsystem). This ability to draw from the United States electrical grid to meet the energy requirements for the brine concentration plants explains the difference in the $CO_2$ emissions. The GHI ranges from 3.9 to 6 kW/(m$^2$ d) with an average of 4.6. The northern USA has the lowest GHI, and the southwest has the highest GHI. Furthermore, continued decarbonization of the US electrical grid could enable these impacts to decrease further.

For the social criterion (Table S11), water stress levels range from 0 (low or <10% risk) to 5 (extremely high or >80% risk)


https://doi.org/10.1021/acs.est.2c05462
Environ. Sci. Technol. XXXX, XXX, XXX−XXX

with an average of 2. A high water stress indicates that the system provides greater benefit to the nearby cities. The percentage of water supplied to nearby cities ranges from 1.1% to 34.4% with an average of 10%. The percentage of supply depends on the total population of the nearby cities to a brine concentration plant and the amount of freshwater produced by the same plant. From the GIS analysis, the 21 brine concentration plants could provide freshwater to 196 million people consuming 0.34 $m^3$ per day for indoor home use per person.[58,64,83] The water supply only considers home indoor use per person. Supplying freshwater from the brine concentration plant to nearby cities with low population increases the total supply percentage of the plant and the value of this subcriterion, as there are fewer people consuming water.

**Relevance of Subcriterion for Decision Making.** The weighting based on Shannon entropy provides the relative importance of each subcriterion within each main criterion (first row in Tables S12−S15). For the thermodynamic criterion, the second-law efficiency has a weight of 0.78. This suggests that the second-law efficiency is the subcriterion with the lowest entropy and largest diversity in the thermodynamic criterion. In information theory, a lower entropy indicates that the subcriterion has low uncertainty when it is compared with the alternatives (here brine concentration plant locations). The Shannon entropy weighting assigns greater importance, and therefore weight, to subcriteria with low uncertainty. The specific entropy generation subcriterion has a weight of 0.15, a recovery ratio of 0.03, and an SEC of 0.04. The recovery ratio has the lowest weight, as the subcriterion does not vary significantly among the different locations, due the fixed outlet brine salinity for a minimal liquid discharge condition (260 g/kg). A subcriterion that does not have significant variability does not contribute to the decision making.[84] Similarly, the SEC has a low weight, due to the insignificant variation due to the specific pumping and compression energy requirements by the system. With objective weighting, it is clear that the relevance of SEC and RR is insignificant, while the thermodynamic efficiency is significant.

For the economic criterion, the transportation cost of the intake and supply have weights of 0.57 and 0.41, respectively. This suggests that the transportation cost is the most important economic aspect with the lowest entropy in the economic criterion. The LCOW has a weight of 0.03 and a land cost of 0. The LCOW has a lower weight due the low variation of capital and operation costs in comparison with the difference between transportation costs. Similarly, land cost has a weight of close to 0 since the change in land cost is less diverse than transportation, increasing its entropy. Objective weighting allows one to conclude that, when comparing the same system at different locations, the LCOW relevance decreases, increasing the importance of the transportation of the feed and product. This highlights the importance for further optimization models aiming at allocating the brine concentration plants in the studied prioritized regions.

For the environmental criterion, the $CO_2$ emissions and the GHI have weights of 0.64 and 0.36, respectively. $CO_2$ emissions have a high variation in every location due the difference in the SEC and the carbon intensity associated with every state. Both parameters explain the large relevance of this subcriterion compared with the GHI, which is not directly related with the system's operation, but has a potential for being renewably driven.

For the social criterion, the water stress level and percentage of water supply to nearby cities have weights of 0.43 and 0.57, respectively, meaning that these subcriteria are the most important social aspects with the lowest entropy in the social criterion. The specific area of the evaporator has a weight of 0, meaning that is not relevant for decision making. The different levels of water stress evaluated in every potential location indicate that this subcriterion is relevant to decision making. The percentage of the supply has a high weight due to the density of the population in nearby cities and the amount of freshwater produced by the brine concentration system.

The overall weight of every subcriterion in an equal priority case (second row in Tables S12−S15) provides the relevance of every subcriterion to the decision making when there are no preferences for thermodynamic, economic, environmental, or social consideration (weight per main criterion equals 0.25). Second-law efficiency has a higher weight of 0.2 followed by $CO_2$ emissions, percentage of supply, transportation cost of intake, water stress, transportation cost of supply, GHI, and specific entropy generation with weights of 0.16, 0.14, 0.14, 0.11, 0.1, 0.09, and 0.04, respectively. Recovery ratio, SEC, land cost, and specific area of the evaporator had weights of below 1%, meaning that for a equal-priority case these subcriteria are not relevant in decision making. This is due to the high entropy of these subcriteria among potential locations compared with the differences presented by other subcriteria.

For the equal-priority case (Figure 4), the system installed in Florida (centroid 6 - FL) ranks in first place with a closeness

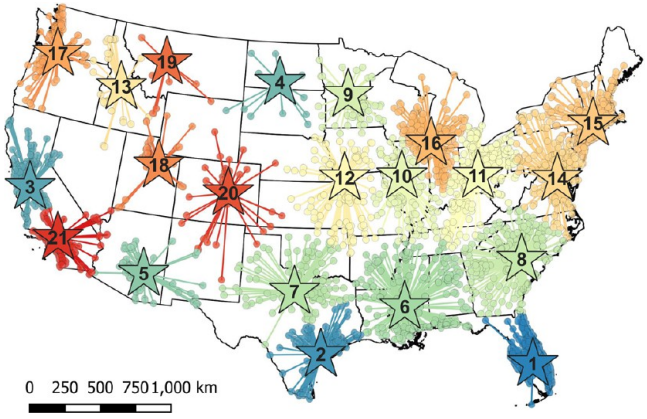


**Figure 4.** Locations ranked from highest to lowest potential based on equal weights for thermodynamic, economic, environmental, and social parameters criteria. Every cluster's centroid is connected to nearby major cities for supplying the produced freshwater, representing the potential population benefit by the installation of a brine concentration plant. The assignation of population to a centroid is made through a nearest distance to hub analysis.

coefficient of 0.87. In this location, the brine concentration plant has a higher capacity for supplying freshwater to nearby cities, with a percentage of freshwater supplied for indoor home use of 34%. The plant location is in a region under a high level of water stress (40−80%). The brine concentration plant has a second-law efficiency of 13.17%, which is an average value compared with other locations, and a low transportation cost for the intake from nearby desalination plants and supply to nearby cities (0.1 and 0.2 cent/$m^3$). Both transportation costs in this location are in the first quartile


https://doi.org/10.1021/acs.est.2c05462
Environ. Sci. Technol. XXXX, XXX, XXX−XXX

(Q1) in comparison with the transportation costs of other locations, meaning that they are in the lowest 25% value in this study. This location has a high GHI, increasing the renewable energy integration, but the $CO_2$ emissions are in the average range with 2.6 kg $CO_2/(m^3\ d)$. The high value of the social subcriteria, low transportation cost, high renewable potential, and the average second-law efficiency explain the high rank of this plant despite the average level of $CO_2$ emissions.

The system installed in Texas (centroid 2 - TX) ranks in second place with a closeness coefficient of 0.744. In this location, the brine concentration plant has the capacity for supplying freshwater to nearby cities equals to 15% of the indoor home use requirements. The plant location is in a region under low−medium water stress (10−20%). The brine concentration plant has a second-law efficiency of 17%, which is above average and is in the third quartile (Q3) in comparison with other locations, meaning that this location has a second-law efficiency in the highest 75% of the values reported by the brine concentration plants in other locations. The transportation cost of the intake from nearby desalination plants of 0.7 cents/$m^3$ corresponds to the lowest quartile (Q1), while the transportation cost of supplying to nearby cities cost is similar to the median values in comparison with other locations (0.012 cent/$m^3$). This location has a high GHI and the $CO_2$ emissions are close to the first quartile with 2.14 kg $CO_2/(m^3\ d)$, meaning that the environmental parameters favor the installation of the brine concentration system in this location.

The system installed in California (centroid 0 - CA) ranks in third place with a closeness coefficient of 0.739. In this location, the brine concentration plant has the capacity of supplying freshwater to nearby population equal to 9.8% of the indoor home use requirements. The plant location is in a region under a extreme level of water stress (>80%). The brine concentration plant has a second-law efficiency of 15.2%, which is above the average of all the potential locations. The transportation cost of intake from nearby desalination plants of 2 cents/$m^3$ is in the median level, while the transportation cost of supplying to nearby cities is below average but greater than the median (3.5 cents/$m^3$). This location has a high GHI and average $CO_2$ emissions (2.28 kg $CO_2/(m^3\ d)$). The second-law efficiency and the high water stress level in the region explain the high position of this location.

The system installed in North Dakota (centroid 3 - ND) ranks in fourth place with a closeness coefficient of 0.738. In this location, the brine concentration plant has a capacity of supplying freshwater to nearby population equal to 30% of the indoor home use requirements. The plant location is in a region under a low level of water stress (<10%). The brine concentration plant has a second-law efficiency of 10%, which is below the average of all the potential locations. The transportation cost of intake from nearby desalination plants of 0.9 cent/$m^3$ is close to the first quartile value (0.7 cent/$m^3$) and 2 times lower than the median, while the transportation cost of supplying to nearby cities of 2.7 cents/$m^3$ is 2-fold higher than the median. This means that the transportation cost in this location is greater than the lower 25% values reported in other locations but lower than the average value. This location has a low GHI and $CO_2$ emissions of 3.03 kg $CO_2/(m^3\ d)$, which is close to the maximum value reported (3.1 kg $CO_2/(m^3\ d)$ in Utah - UT cluster). The high $CO_2$ intensity of North Dakota's grid explain the large value in the environmental parameter. The percentage of freshwater supplied for indoor home usage explains the position of this location compared with the other options.

The system installed in south California (centroid 13 - CA2) ranks in last place with a closeness coefficient of 0.33. In this location, the brine concentration plant has the capacity of supplying freshwater to nearby population equal to 27% of the indoor home use requirements. The plant location is in a region under an extreme level of water stress (>80%). The brine concentration plant has a second-law efficiency of 14.8%, which is above average, and the largest transportation cost for both intake from nearby desalination plants and supply to nearby cities (5.9 and 6.4 cents/$m^3$). This location has a high GHI and average $CO_2$ emissions (2.29 kg $CO_2/(m^3\ d)$). The high transportation cost compared with other options explains the low rank of this alternative. This economic constraint overcomes the social and environmental potential of this location for an equal- priority case. The results for this region, considering the large amount of freshwater produced, suggest that a single system treating large amounts of brine is not a suitable strategy and, therefore, this region must be divided into subregions.

**Influence of Priority on Decision-Making Criteria.** The equal-priority case ranks the potential location objectively due to the use of the data entropy for weighting. Here, the most relevant subcriterion in decision making is the subcriterion with the highest variability among locations. Changing the weight of the main criteria manually ($\omega$) adds subjectivity to the analysis, giving preference to one main criterion among the others. The change in the main criteria weight has a direct impact on the global weight of every subcriterion in decision making.

In the thermodynamic priority case ($\omega_1 = 0.5$), the second-law efficiency is the most influential subcriterion with a global weight of 0.39. $CO_2$ emissions with a global weight of 0.11 follows as the second most influential (Table S12). Under this scenario (Figure S7), the brine concentration plants located in Florida and Texas (centroids 6 and 2, FL and TX) rank in first and second place again. The brine concentration plants located in Mississippi (centroid 10, MS ranked sixth in the equal-priority case) ranks in third place, indicating that this location had better performance from a thermodynamic point of view. The brine concentration plant in California drops from third to fourth place, while that in North Dakota falls down to the seventh position, meaning that the thermodynamic performance of the system is low compared with other options. The brine concentration plant located in south California (centroid 13, CA-2) remains in the last position under this scenario.

In the economic priority case ($\omega_2 = 0.5$), the transportation cost of the intake from desalination plants is the most influential subcriterion with a global weight of 0.28. The transportation cost of supplying the produced water to nearby cities with a weight of 0.2 follows as the second most influential (Table S13). The LCOW global weight increases to 0.011 but still is not comparable with transportation costs. This does not means that the transportation cost is higher than the LCOW but that the diversity of the subcriterion in every location is higher, supposing a large influence in decision making. Under this scenario (Figure S8), the systems located in Florida and Texas (centroids 6 and 2, Fl and TX) rank in first and second place again. The brine concentration plant located in North Dakota (centroid 3, ND) ranks in third place, displacing the plant installed in California (centroid 0, CA). This is due to the reduced costs of the plant installed in North


https://doi.org/10.1021/acs.est.2c05462
Environ. Sci. Technol. XXXX, XXX, XXX−XXX

**Table 1. Priority for Every Studied Regions under Different Priority Weights in Main Criteria[a]**

| location | equal priority | thermodynamics priority | economics priority | environmental priority | social priority |
|---|---|---|---|---|---|
| Florida (FL) | 1 | 1 | 1 | 1 | 1 |
| Texas (TX) | 2 | 2 | 2 | 2 | 7 |
| California (CA) | 3 | 4 | 4 | 3 | 5 |
| North Dakota (ND) | 4 | 8 | 3 | 12 | 2 |
| Arizona (AZ) | 5 | 5 | 5 | 4 | 6 |
| Mississippi (MS) | 6 | 3 | 6 | 6 | 9 |
| Texas (TX-2) | 7 | 16 | 9 | 7 | 8 |
| South Carolina (SC) | 8 | 7 | 7 | 5 | 11 |
| Minnesota (MN) | 9 | 9 | 8 | 10 | 10 |
| Illinois (IL-2) | 10 | 11 | 10 | 9 | 13 |
| Ohio (OH) | 11 | 6 | 11 | 15 | 15 |
| Missouri (MO) | 12 | 17 | 12 | 18 | 12 |
| Idaho (ID) | 13 | 10 | 20 | 8 | 3 |
| Maryland (MD) | 14 | 13 | 13 | 16 | 17 |
| Connecticut (CT) | 15 | 12 | 14 | 11 | 18 |
| Illinois (IL) | 16 | 15 | 15 | 14 | 21 |
| Washington (WA) | 17 | 14 | 16 | 13 | 20 |
| Utah (UT) | 18 | 20 | 17 | 20 | 16 |
| Montana (MT) | 19 | 18 | 18 | 17 | 19 |
| Colorado (CO) | 20 | 19 | 19 | 19 | 14 |
| California (CA-2) | 21 | 21 | 21 | 21 | 4 |

[a]Locations are ordered based on equal priority in the main criteria.

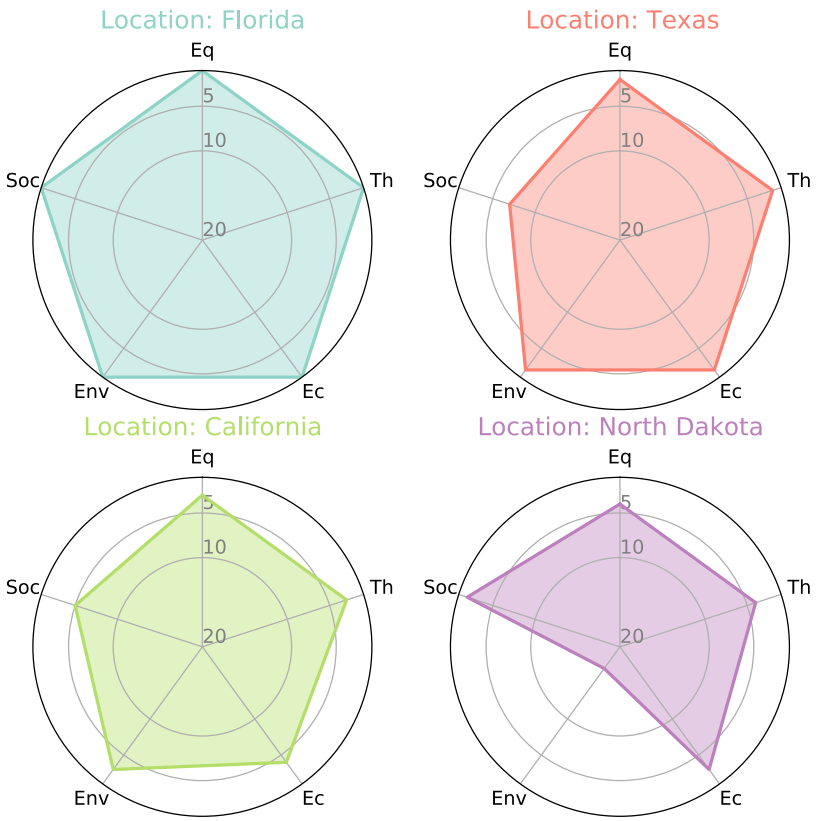


**Figure 5.** Sensitivity analysis for the top four locations in the equal-priority case (Eq). The sensitivity analysis evaluates the position where the location gets more when the priority/weight increases for thermodynamic (Th), economic (Ec), environmental (Env), and social (Soc) parameters.

Dakota (transportation, but also LCOW and Land). The brine concentration plants located in south California (centroid 13, CA-2) remains in the last position under this scenario.

In the environmental priority case ($\omega_3$ = 0.5), $CO_2$ emissions are the most influential subcriterion with a global weight of 0.32. GHI with a global weight of 0.18 follows as the second most influential (Table S14). Second-law efficiency is still an influential subcriterion with a global weight of 0.13. Under this scenario (Figure S9), the brine concentration plants located in Florida and Texas (centroids 6 and 2, FL and TX) rank in first and second place again. The brine concentration plant located in Arizona (centroid 5, AZ) ranks in fourth place,


https://doi.org/10.1021/acs.est.2c05462
Environ. Sci. Technol. XXXX, XXX, XXX−XXX

displacing North Dakota to the twelfth position (ranked fourth in the equal-priority case). The brine concentration plant located in Arizona has lower $CO_2$ emissions and higher GHI. Additionally, these subcriteria do not favor the system located in North Dakota. The brine concentration plant located in south California (centroid 13, CA-2) remains in the last position under this scenario.

In the social priority case ($\omega_4 = 0.5$), the percentage of water supplied to nearby cities is the most influential subcriterion with a global weight of 0.28. Water stress level with a global weight of 0.22 follows as the second most influential (Table S15). Second-law efficiency and $CO_2$ emissions are still influential subcriteria with global weights of 0.13 and 0.11, respectively. Under this scenario (Figure S10), the brine concentration plant located in Florida (centroid 6, FL) ranks in first place again. The plant located in North Dakota (centroid 3, ND) ranks in second place (ranked fourth in the equal-priority case) due to the large percentage of freshwater supplied to nearby cities for indoor home use (30%), which has an increased influence on decision making under this scenario. Social considerations do not favor the plants located in Texas or California (centroids 2 and 0, TX, CA) ranking in fifth and seventh places. When the weight to the defined social parameters is increased, the brine concentration plants located in Idaho and south California (centroid 7 and 13, ID and CA-2) rank in third and fourth places (from thirteenth and last positions in the equal-priority case). These two points have the biggest change in ranking for all different priority cases. This is due the fact that the systems in both location have a large capacity for supplying freshwater to nearby cities (27%), which is higher than the majority of locations in this analysis. South California has an extreme level of water stress compared with Idaho; however the transportation cost is 4 and 3 times higher, explaining the difference in preferences under this scenario. This difference in ranking positions when a defined criterion increases its preference (weight) indicates that decision making based only on a specific criterion can possibly lead to the selection of a location where the system does not have a good overall performance, promoting the need for a multicriteria decision analysis (Table 1).

**Best Priority Locations for Brine Concentrators.** A sensitivity analysis for the best four locations in the equal-priority case evaluates the consistency of the ranking changes when considering priority cases for a main criterion. The weight of the main criterion $\omega$ varies from the equal-priority case ($\omega = 0.25$) and passes thorugh the priority case ($\omega_i = 0.5$) up to 0.7 (extreme priority) by a factor of 0.05. The mode value provides the ranking that every location obtained the most during the sensitivity analysis (Figure S11).

For every priority case, the brine concentration plant installed in Florida (centroid 6, FL) ranks in first place the most, independently of the weights assigned to the main criteria (Figure 5). This means that this location has the greatest potential for implementing the studied system, providing benefit under all the main criteria parameters. From a geographic analysis in this location, the brine concentration plant treats brine coming from nearby desalination plants located near the coast and uses mostly brackish water as feedwater (52%), followed by wastewater (24%), seawater (11%), river water (10%), and pure water (2%). The LCOW of the brine concentration plant in this region (1.8 $/m$^3$) is comparable to those of deep-well injection (2−2.8 $/m$^3$) and land irrigation (1−1.6 $/m$^3$) and higher than surface discharge to the sea (0.4−0.8 $/m$^3$). Considering the closeness to the coast (32 km on average to the coastline), discharge brine treatment to the sea represents an economic alternative in this area, but the low salinity of the total brine produced by the nearby desalination plants (~30 g/kg) offers to the studied system an opportunity to increase the production of freshwater for supplying the nearby population.

The brine concentration plant installed in Texas (centroid 2, TX), ranked second in the equal-priority case, ranks consistently the most in second place for every priority case, with the exception of the social priority sensitivity analysis. Here, the most repeated position is the seventh place, indicating that the system located in Texas does not provide a benefit under the social parameters considered in this work. While it has the capacity for providing a 15% of the indoor home water demand from nearby cities, the plant location is in a low water stress region, decreasing its ranking. From a geographic analysis in this location, the brine concentration plant treats brine coming from nearby desalination plants located near the coast and uses mostly brackish water as feedwater (58%), followed by river water (34%), seawater (7%), wastewater (1%), and pure water (0%). The LCOW of the brine concentration plant in this region (0.87 $/m$^3$) is lower than those of deep-well injection and land irrigation and comparable to that of surface discharge to the sea. The desalination plant connected to the brine concentration plant in this region is far from the coast (100 km on average from the coastline) compared with the plants providing brine to the system located in Florida. The salinity of the total brine produced by the nearby desalination plant is higher than that of the plant located in Florida (~43 g/kg) but still offers to the studied system an opportunity to increase the production of freshwater for supplying the nearby population, in comparison with conventional brine rejection to water surfaces.

The brine concentration plant installed in North California (centroid 0, CA), ranked third in the equal-priority case, ranks the most in third for the thermodynamic and environmental sensitivity analysis, fourth for economic priority, and fifth for social. The system in this location is consistently a good alternative for decision making, providing benefits under different criteria, in comparison with other locations. From a geographic analysis in this location, the brine concentration plant treats brine coming from nearby desalination plants located near the coast and uses mostly brackish water as feedwater (56%), followed by wastewater (24%), seawater (11%), river water (6%), and pure water (2%). The desalination plant connected to the brine concentration plant on this region is far from the coast (107 km in average from the coastline). The salinity of the total brine produced by the nearby desalination plants is similar to seawater levels (~37 g/kg), offering to the studied system an opportunity to increase the production of freshwater for supplying the nearby population, in comparison with conventional brine rejection to water surfaces.

The brine concentration plant installed in North Dakota (centroid 3, ND), ranked fourth in the equal priority case, ranks the most in third for the economic, second for the social, and seventeenth for the environmental sensitivity analysis. A special case occurs in the thermodynamic sensitivity analysis, where there is no ranking value repeated, going from fourth position to seventheenth with a median of eightyh (Figure S11d). In this case, the best ranking obtained is considered (Figure 5). The low ranking in the environmental analysis is


https://doi.org/10.1021/acs.est.2c05462
Environ. Sci. Technol. XXXX, XXX, XXX−XXX

due to the low GHI available in the area compared with other potential locations and the high $CO_2$ emissions associated with the system. The carbon intensity in North Dakota in 2018 is one of the highest in the USA, explaining this result. From a geographic analysis of this location, the brine concentration plant treats brine coming from nearby desalination plants located near the coast and using mostly river water as feedwater (78%), followed by brackish water (21%), wastewater (1%), pure water (0%), and seawater (0%). The desalination plant connected to the brine concentration plant in this region is far from the coast (695 km in average to the coastline), surpassing the critical threshold for the conveyance of water, making surface water discharge an unfeasible option in this location. Since the majority of the plants near the brine concentration system in this location treat river water, the salinity of the total brine produced by the nearby desalination plants is lower than seawater levels (~22 g/kg), offering to the studied system a high opportunity for increasing the production of freshwater for supplying the nearby population, in comparison with conventional brine rejection to water surfaces.

## ■ ASSOCIATED CONTENT

### Supporting Information

The Supporting Information is available free of charge at https://pubs.acs.org/doi/10.1021/acs.est.2c05462.

Details of the computational model, priority case maps, and correlations (PDF)

## ■ AUTHOR INFORMATION


### Corresponding Author

**Marta C. Hatzell** − *George W. Woodruff School of Mechanical Engineering and Department of Chemical and Biomolecular Engineering, Georgia Institute of Technology, Atlanta, Georgia 30313, United States;* orcid.org/0000-0002-5144-4969; Phone: +1 (404) 385 4503; Email: marta.hatzell@me.gatech.edu

### Author

**Rodrigo A. Caceres Gonzalez** − *George W. Woodruff School of Mechanical Engineering, Georgia Institute of Technology, Atlanta, Georgia 30313, United States;* orcid.org/0000-0003-3682-6130

Complete contact information is available at: https://pubs.acs.org/10.1021/acs.est.2c05462


### Notes

The authors declare no competing financial interest.

## ■ ACKNOWLEDGMENTS

The authors were supported by the National Science Foundation under grant no. 1821843. R.A.C.G. acknowledges support from the National Agency for Research and Development (ANID)/Scholarship Program/DOCTORADO BECAS CHILE/2018-72190312.

## ■ REFERENCES


(1) van Vliet, M. T.; Jones, E. R.; Flörke, M.; Franssen, W. H.; Hanasaki, N.; Wada, Y.; Yearsley, J. R. Global water scarcity including surface water quality and expansions of clean water technologies. *Environmental Research Letters* **2021**, *16*, 024020.

(2) Munia, H. A.; Guillaume, J. H.; Wada, Y.; Veldkamp, T.; Virkki, V.; Kummu, M. Future transboundary water stress and its drivers under climate change: a global study. *Earth's future* **2020**, *8*, e2019EF001321.

(3) GWI,*DesalData Database*. Available at: https://www.desaldata.com/, Accessed: 2021-03-23.

(4) Jones, E.; Qadir, M.; van Vliet, M. T.; Smakhtin, V.; Kang, S.-m The state of desalination and brine production: A global outlook. *Sci. Total Environ.* **2019**, *657*, 1343−1356.

(5) Darre, N. C.; Toor, G. S. Desalination of water: a review. *Current Pollution Reports* **2018**, *4*, 104−111.

(6) Panagopoulos, A.; Haralambous, K.-J.; Loizidou, M. Desalination brine disposal methods and treatment technologies-A review. *Sci. Total Environ.* **2019**, *693*, 133545.

(7) Panagopoulos, A.; Haralambous, K.-J. Environmental impacts of desalination and brine treatment-Challenges and mitigation measures. *Mar. Pollut. Bull.* **2020**, *161*, 111773.

(8) Tong, T.; Elimelech, M. The global rise of zero liquid discharge for wastewater management: drivers, technologies, and future directions. *Environ. Sci. Technol.* **2016**, *50*, 6846−6855.

(9) Panagopoulos, A. Techno-economic assessment of minimal liquid discharge (MLD) treatment systems for saline wastewater (brine) management and treatment. *Process Safety and Environmental Protection* **2021**, *146*, 656−669.

(10) Wang, Z.; Feng, D.; Chen, Y.; He, D.; Elimelech, M. Comparison of energy consumption of osmotically assisted reverse osmosis and low-salt-rejection reverse osmosis for brine management. *Environ. Sci. Technol.* **2021**, *55*, 10714−10723.

(11) Panagopoulos, A.; Haralambous, K.-J. Minimal Liquid Discharge (MLD) and Zero Liquid Discharge (ZLD) strategies for wastewater management and resource recovery−Analysis, challenges and prospects. *Journal of Environmental Chemical Engineering* **2020**, *8*, 104418.

(12) Boo, C.; Billinge, I. H.; Chen, X.; Shah, K. M.; Yip, N. Y. Zero liquid discharge of ultrahigh-salinity brines with temperature swing solvent extraction. *Environ. Sci. Technol.* **2020**, *54*, 9124−9131.

(13) Finnerty, C.; Zhang, L.; Sedlak, D. L.; Nelson, K. L.; Mi, B. Synthetic graphene oxide leaf for solar desalination with zero liquid discharge. *Environ. Sci. Technol.* **2017**, *51*, 11701−11709.

(14) Odu, S. O.; van der Ham, A. G.; Metz, S.; Kersten, S. R. Design of a process for supercritical water desalination with zero liquid discharge. *Ind. Eng. Chem. Res.* **2015**, *54*, 5527−5535.

(15) Shi, Y.; Zhang, C.; Li, R.; Zhuo, S.; Jin, Y.; Shi, L.; Hong, S.; Chang, J.; Ong, C.; Wang, P. Solar evaporator with controlled salt precipitation for zero liquid discharge desalination. *Environ. Sci. Technol.* **2018**, *52*, 11822−11830.

(16) Chen, Y.; Davis, J. R.; Nguyen, C. H.; Baygents, J. C.; Farrell, J. Electrochemical ion-exchange regeneration and fluidized bed crystallization for zero-liquid-discharge water softening. *Environ. Sci. Technol.* **2016**, *50*, 5900−5907.

(17) Finnerty, C. T.; Menon, A. K.; Conway, K. M.; Lee, D.; Nelson, M.; Urban, J. J.; Sedlak, D.; Mi, B. Interfacial solar evaporation by a 3D graphene oxide stalk for highly concentrated brine treatment. *Environ. Sci. Technol.* **2021**, *55*, 15435−15445.

(18) Arias-Paić, M. S.; Korak, J. A. Forward osmosis for ion exchange waste brine management. *Environmental Science & Technology Letters* **2020**, *7*, 111−117.

(19) Peters, C. D.; Li, D.; Mo, Z.; Hankins, N. P.; She, Q. Exploring the Limitations of Osmotically Assisted Reverse Osmosis: Membrane Fouling and the Limiting Flux. *Environ. Sci. Technol.* **2022**, *56*, 6678.

(20) Bartholomew, T. V.; Siefert, N. S.; Mauter, M. S. Cost optimization of osmotically assisted reverse osmosis. *Environ. Sci. Technol.* **2018**, *52*, 11813−11821.

(21) Chen, X.; Yip, N. Y. Unlocking high-salinity desalination with cascading osmotically mediated reverse osmosis: Energy and operating pressure analysis. *Environ. Sci. Technol.* **2018**, *52*, 2242−2250.

(22) Grubert, E. A.; Stillwell, A. S.; Webber, M. E. Where does solar-aided seawater desalination make sense? A method for identifying sustainable sites. *Desalination* **2014**, *339*, 10−17.
(23) Eckert, S.; Giger, M.; Messerli, P. Contextualizing local-scale point sample data using global-scale spatial datasets: Lessons learnt from the analysis of large-scale land acquisitions. *Applied geography* **2016**, *68*, 84−94.
(24) Ziolkowska, J. R.; Reyes, R. Geospatial analysis of desalination in the US−An interactive tool for socio-economic evaluations and decision support. *Applied Geography* **2016**, *71*, 115−122.
(25) Thorslund, J.; van Vliet, M. T. a global dataset of surface water and groundwater salinity measurements from. *Scientific Data* **2020**, *7*, 1−11.
(26) Xu, X.; Ness, J. E.; Miara, A.; Sitterley, K. A.; Talmadge, M.; O'Neill, B.; Coughlin, K.; Akar, S.; Edirisooriya, E. T.; Kurup, P.; Rao, N.; Macknick, J.; Stokes-Draut, J. R.; Xu, P. Analysis of Brackish Water Desalination for Municipal Uses: Case Studies on Challenges and Opportunities. *ACS ES&T Engineering* **2022**, *2*, 306−322.
(27) Quon, H.; Sperling, J.; Coughline, K.; Greene, D.; Miara, A.; Akar, S.; Talmadge, M.; Stokes-Draut, J. R.; Macknick, J.; Jiang, S. Pipe Parity Analysis of Seawater Desalination in the United States: Exploring Costs, Energy, and Reliability via Case Studies and Scenarios of Emerging Technology. *ACS ES&T Engineering* **2022**, *2*, 434−445.
(28) Wang, J.-J.; Jing, Y.-Y.; Zhang, C.-F.; Zhao, J.-H. Review on multi-criteria decision analysis aid in sustainable energy decision-making. *Renewable and sustainable energy reviews* **2009**, *13*, 2263−2278.
(29) Afify, A. Prioritizing desalination strategies using multi-criteria decision analysis. *Desalination* **2010**, *250*, 928−935.
(30) Ghassemi, S. A.; Danesh, S. A hybrid fuzzy multi-criteria decision making approach for desalination process selection. *Desalination* **2013**, *313*, 44−50.
(31) Aliewi, A.; El-Sayed, E.; Akbar, A.; Hadi, K.; Al-Rashed, M. Evaluation of desalination and other strategic management options using multi-criteria decision analysis in Kuwait. *Desalination* **2017**, *413*, 40−51.
(32) Vishnupriyan, J.; Arumugam, D.; Kumar, N. M.; Chopra, S. S.; Partheeban, P. Multi-criteria decision analysis for optimal planning of desalination plant feasibility in different urban cities in India. *Journal of Cleaner Production* **2021**, *315*, 128146.
(33) Mohamed, S. A. Application of geo-spatial analytical hierarchy process and multi-criteria analysis for site suitability of the desalination solar stations in Egypt. *Journal of African Earth Sciences* **2020**, *164*, 103767.
(34) Dawoud, O.; Ahmed, T.; Abdel-Latif, M.; Abunada, Z. A spatial multi-criteria analysis approach for planning and management of community-scale desalination plants. *Desalination* **2020**, *485*, 114426.
(35) Boroushaki, S. Entropy-based weights for multicriteria spatial decision-making. *Yearbook of the Association of Pacific Coast Geographers* **2017**, *79*, 168−187.
(36) Lienhard, J. H.; Mistry, K. H.; Sharqawy, M. H.; Thiel, G. P.*Desalination Sustainability A Technical, Socioeconomic, and Environmental Approach*; Elsevier: 2017; Chapter 4, pp 127−206.
(37) Zheng, Y.; Caceres Gonzalez, R. A.; Hatzell, K. B.; Hatzell, M. C. Large-scale solar-thermal desalination. *Joule* **2021**, *5*, 1971−1986.
(38) Klein, S. A.; Nellis, G.*EES, Engineering Equation Solver*. 2017; http://www.fchart.com/ees/.
(39) Mistry, K. H.; McGovern, R. K.; Thiel, G. P.; Summers, E. K.; Zubair, S. M.; Lienhard, J. H. Entropy generation analysis of desalination technologies. *Entropy* **2011**, *13*, 1829−1864.
(40) Thiel, G. P.; Tow, E. W.; Banchik, L. D.; Chung, H. W.; Lienhard, J. H. Energy consumption in desalinating produced water from shale oil and gas extraction. *Desalination* **2015**, *366*, 94−112.
(41) Warsinger, D. M.; Mistry, K. H.; Nayar, K. G.; Chung, H. W.; Lienhard, J. H. Entropy generation of desalination powered by variable temperature waste heat. *Entropy* **2015**, *17*, 7530−7566.
(42) Lu, Y.; Liao, A.; Hu, Y. The design of reverse osmosis systems with multiple-feed and multiple-product. *Desalination* **2012**, *307*, 42−50.
(43) Wang, L.; Violet, C.; DuChanois, R. M.; Elimelech, M. Journal of Chemical Education. *J. Chem. Educ.* **2020**, *97*, 4361−4369.
(44) Nafey, A.; Sharaf, M. Combined solar organic Rankine cycle with reverse osmosis desalination process: energy, exergy, and cost evaluations. *Renewable Energy* **2010**, *35*, 2571−2580.
(45) El-Dessouky, H. T.; Ettouney, H. M.*Fundamentals of salt water desalination*; Elsevier: 2002; pp 211−270.
(46) Pitzer, K. S.; Peiper, J. C.; Busey, R. Thermodynamic properties of aqueous sodium chloride solutions. *J. Phys. Chem. Ref. Data* **1984**, *13*, 1−102.
(47) Sparrow, B. S. Empirical equations for the thermodynamic properties of aqueous sodium chloride. *Desalination* **2003**, *159*, 161−170.
(48) Generous, M. M.; Qasem, N. A.; Qureshi, B. A.; Zubair, S. M. A comprehensive review of saline water correlations and data-Part I: Thermodynamic properties. *Arabian Journal for Science and Engineering* **2020**, 1−60.
(49) Qasem, N. A.; Generous, M. M.; Qureshi, B. A.; Zubair, S. M. A Comprehensive Review of Saline Water Correlations and Data: Part II−Thermophysical Properties. *Arabian Journal for Science and Engineering* **2021**, 1−39.
(50) Mistry, K. H.; Lienhard, J. H. Effect of nonideal solution behavior on desalination of a sodium chloride (NaCl) solution and comparison to seawater. *Mechanical Engineering Congress and Exposition* **2012**, *45226*, 1509−1523.
(51) Nayar, K. G.; Fernandes, J.; McGovern, R. K.; Al-Anzi, B. S.; Lienhard, J. H. Cost and energy needs of RO-ED-crystallizer systems for zero brine discharge seawater desalination. *Desalination* **2019**, *457*, 115−132.
(52) Chemical Engineering: Essential for the CPI Professional, 2021 CEPCI UPDATES: SEPTEMBER (PRELIM.) AND AUGUST (FINAL). https://www.chemengonline.com/2021-cepci-updates-september-prelim-and-august-final/, 2021; accessed May 24, 2022.
(53) Vatavuk, W. M. Updating the CE plant cost index. *Chemical Engineering* **2002**, *109*, 62−70.
(54) Murthy, G. S.*Biomass, Biofuels, Biochemicals*; Elsevier: 2022; pp 17−32.
(55) Rao, P.; Morrow, W. R., III; Aghajanzadeh, A.; Sheaffer, P.; Dollinger, C.; Brueske, S.; Cresko, J. Energy considerations associated with increased adoption of seawater desalination in the United States. *Desalination* **2018**, *445*, 213−224.
(56) Solargis, Terrain elevationGlobal Solar Atlas. Available at: https://datacatalog.worldbank.org/search/dataset/0037910, accessed 2021-06.
(57) (US) EIA, Energy-Related CO2 Emission Data Tables. Available at: https://www.eia.gov/environment/emissions/state/, accessed 2021-06.
(58) USGS,*How much water do I use at home each day*? Available at: https://www.usgs.gov/special-topic/water-science-school/science/water-qa-how-much-water-do-i-use-home-each-day?qt-science_center_objects/0#qt-science_center_objects, accessed 2021-09-30.
(59) QGIS Development Team*QGIS Geographic Information System*; QGIS Association: 2021.
(60) Sengupta, M.; Xie, Y.; Lopez, A.; Habte, A.; Maclaurin, G.; Shelby, J. The national solar radiation data base (NSRDB). *Renewable and Sustainable Energy Reviews* **2018**, *89*, 51−60.
(61) Hofste, R. W.; Kuzma, S.; Walker, S.; Sutanudjaja, E. H.; Bierkens, M. F.; Kuijper, M. J.; Faneca Sanchez, M.; Van Beek, R.; Wada, Y.; Galvis Rodríguez, S.; Reig, P.*Aqueduct 3.0: Updated decision-relevant global water risk indicators*; World Resources Institute: 2019,.
(62) Nolte, C. High-resolution land value maps reveal underestimation of conservation costs in the United States. *Proc. Natl. Acad. Sci. U. S. A.* **2020**, *117*, 29577−29583.
(63) US EIA*State Electricity Profiles*. Available at: https://www.eia.gov/electricity/state/, accessed 2021-06.


https://doi.org/10.1021/acs.est.2c05462
Environ. Sci. Technol. XXXX, XXX, XXX−XXX

(64) ESRI*USA Major Cities*. Available at: https://hub.arcgis.com/datasets/esri::usa-major-cities/about, accessed 2021-06.
(65) Soliman, A.; Alharbi, A. G.; Sharaf Eldean, M. A. Techno-Economic Optimization of a Solar−Wind Hybrid System to Power a Large-Scale Reverse Osmosis Desalination Plant. *Sustainability* **2021**, *13*, 11508.
(66) Hwang, C.-L.; Yoon, K.*Multiple attribute decision making: a state of the art survey*; Springer-Verlag: 1981; Lecture notes in economics and mathematical systems Vol. *186*; pp 128−141.
(67) Lu, Z.; Broesicke, O. A.; Chang, M. E.; Yan, J.; Xu, M.; Derrible, S.; Mihelcic, J. R.; Schwegler, B.; Crittenden, J. C. Seven approaches to manage complex coupled human and natural systems: A sustainability toolbox. *Environ. Sci. Technol.* **2019**, *53*, 9341−9351.
(68) Gumus, S.; Kucukvar, M.; Tatari, O. Intuitionistic fuzzy multi-criteria decision making framework based on life cycle environmental, economic and social impacts: The case of US wind energy. *Sustainable Production and Consumption* **2016**, *8*, 78−92.
(69) Mostafaeipour, A.; Mohammadi, S. M.; Najafi, F.; Issakhov, A. Investigation of implementing solar energy for groundwater desalination in arid and dry regions: A case study. *Desalination* **2021**, *512*, 115039.
(70) Chamblás, O.; Pradenas, L. Multi-criteria optimization for seawater desalination. *Tecnología y ciencias del agua* **2018**, *9*, 198−212.
(71) Shannon, C. E. A mathematical theory of communication. *Bell system technical journal* **1948**, *27*, 379−423.
(72) Huang, J.Combining entropy weight and TOPSIS method for information system selection.*2008 IEEE conference on cybernetics and intelligent systems*, 2008; pp 1281−1284
(73) Ye, J. Fuzzy decision-making method based on the weighted correlation coefficient under intuitionistic fuzzy environment. *European Journal of Operational Research* **2010**, *205*, 202−204.
(74) Li, X.; Wang, K.; Liu, L.; Xin, J.; Yang, H.; Gao, C. Application of the entropy weight and TOPSIS method in safety evaluation of coal mines. *Procedia engineering* **2011**, *26*, 2085−2091.
(75) Zhu, Y.; Tian, D.; Yan, F. Effectiveness of entropy weight method in decision-making. *Mathematical Problems in Engineering* **2020**, *2020*, 3564835.
(76) Yue, C. Entropy-based weights on decision makers in group decision-making setting with hybrid preference representations. *Applied Soft Computing* **2017**, *60*, 737−749.
(77) Chen, Q.; Burhan, M.; Shahzad, M. W.; Ybyraiymkul, D.; Akhtar, F. H.; Li, Y.; Ng, K. C. A zero liquid discharge system integrating multi-effect distillation and evaporative crystallization for desalination brine treatment. *Desalination* **2021**, *502*, 114928.
(78) Chung, H. W.; Nayar, K. G.; Swaminathan, J.; Chehayeb, K. M.; Lienhard V, J. H. Thermodynamic analysis of brine management methods: zero-discharge desalination and salinity-gradient power production. *Desalination* **2017**, *404*, 291−303.
(79) Rao, P.; Aghajanzadeh, A.; Sheaffer, P.; Morrow, W. R.; Brueske, S.; Dollinger, C.; Price, K.; Sarker, P.; Ward, N.; Cresko, J.*Volume 1: survey of available information in support of the energy-water bandwidth study of desalination systems*, 2016; https://escholarship.org/uc/item/4sw805r2.
(80) Jamil, M. A.; Shahzad, M. W.; Zubair, S. M. A comprehensive framework for thermoeconomic analysis of desalination systems. *Energy conversion and management* **2020**, *222*, 113188.
(81) Cath, T.; Chellam, S.; Katz, L.; Breckenridge, R.; Ellison, K.; Macknick, J.; Monnell, J.; Rao, N.; Sedlak, D.; Stokes-Draut, J.*National Alliance for Water Innovation (NAWI) Technology Roadmap: Resource Extraction Sector*; 2021.
(82) Rabiee, H.; Khalilpour, K. R.; Betts, J. M.; Tapper, N. Energy-water nexus: renewable-integrated hybridized desalination systems. *Polygeneration with polystorage for chemical and energy hubs* **2019**, 409−458.
(83) Ahmad, R.*Water Conservation Programs and Technologies in the USA*; 2008.
(84) Sen, P.; Yang, J.-B.*Multiple criteria decision support in engineering design*; Springer Science & Business Media: 2012; pp 31−33.


https://doi.org/10.1021/acs.est.2c05462
*Environ. Sci. Technol.* XXXX, XXX, XXX−XXX